Received: 30 October 2023 | Revised: 19 January 2024 | Accepted: 8 February 2024

DOI: 10.1002/appl.202300113

RESEARCH ARTICLE

Applied Research

Membrane-based mechanical characterization of screen-printed inks: Deflection analysis of ink layers on polyimide membranes

Eléonore Masarweh[1] | **Mariia Arseenko**[2] | **Philippe Guaino**[2] | **Denis Flandre**[1]

[1]ELEN, ICTeam, UCLouvain, Louvain-la-Neuve, Belgium

[2]Advanced & Smart Surface Solutions, CRM Group, Liège, Belgium

Correspondence
Eléonore Masarweh, ELEN, ICTeam, UCLouvain, Place du Levant, 3, 1348 Louvain-la-Neuve, Belgium.
Email: eleonore.masarweh@uclouvain.be

Funding information
Wallonia Region

Abstract

Measurements of Young's modulus and residual stresses of screen-printed ink layers using a bulge test on coated polyimide-based membranes are proposed in this work. The applied bulge test monitors the deflection of membranes under pressure with interferometry. The obtained Young's modulus ranges from 6 to 8 GPa for a carbon blend-based ink and is around 12 GPa for a silver nanoparticle ink. These values are compared with standard nanoindentation and show good agreement. Besides, the residual stresses range from −4 to 8 MPa for the carbon blend-based ink, while the silver ink is measured around −10 MPa. The use of the membrane-based method underlines the influence of exact deposition and curing conditions on the ink film material properties. The impact of the substrate on the ink layer properties, such as the thickness and its uniformity, is discussed, especially with regard to the heat treatment of the membrane.

KEYWORDS
bulge test, deflection, membranes, residual stress, screen printing, Young's modulus

INTRODUCTION

Processes with lower complexity to produce sensing structures are in line with the global context of technological transitions. Fabrication of devices with hybrid processes between vacuum-based technologies and printed elements opens possibilities to reduce the use of energy-intensive manufacturing steps. To investigate the feasibility of hybrid micro-electromechanical systems (MEMS) with screen-printed ink, knowledge of the material characteristics of thick films [1] is key. This is especially the case for MEMS on membranes, such as pressure sensors. In this work, the mechanical behavior of screen-printed thick films [1] on µm-thick polyimide membranes is analysed to extract the residual stress and Young's Modulus.

Screen-printing deposits layers of functional inks in a liquid or paste form which is then heat-treated. Screen-printed coatings are considered as thick films [1] with thicknesses ranging from 1 to several tens of microns. The electrical properties of the ink are determined by inclusion of the different filler particles in the formulation depending on the target function. These fillers can impact or even dominate the mechanical properties of the ink, depending on the proportion of filler in the dried ink [2–4]. Depending on the type of filler, ink viscosity, and deposition conditions, the observed roughness can go from a few hundreds of nanometers to several microns high [2]. The influence of the substrate partially conditions the ink layer itself through several parameters, among which the wettability that strongly impacts the thickness and the spread [5, 6]. The possible interactions between the ink and the substrate can range from diffusion phenomenons [7] to topology changes linked to for example to spreading [5].

While, in datasheets, the measured characteristics are systematically given along a set of specific depositions and curing conditions [8–10], characteristics such as resistivity can vary along curing conditions [10] and no mechanical characteristics is given except for density [8–10]. Two main types of heat treatment can be found for screen-printing inks in literature: a drying phase at relatively low temperature followed by a sintering at higher temperature, ranging

above 700°C [3, 4] or a curing phase at lower temperature (<200°C) for various durations [8–11]. In the case of the curing bellow 200°C, temperature changes of the order of 10°C can impact the ink mechanical properties such as Young's modulus [11].

Different techniques exist to measure the mechanical properties of such films, each featuring advantages and limitations. In this work, bulge test measurements on polyimide membranes and nanoindentation results are presented.

- The bulge test is based on a thin layer of material that deflects when submitted to a pressure [12–15]. The deflection is monitored and its relation to the pressure yields information on the materials mechanical characteristics. Industrial versions of the bulge test are typically performed on circular thin plates, fully clamped in a chamber setup and put under pressure using a liquid [12]. Similar tests implying membrane deflection to extract material properties of films can be found in the literature [13–17]. Measurement setups often show variations in the deflection-inducing stimulus such as atomic force microscope-based membrane deflection on graphene [16] or simply differential air pressure on solid thin films [13, 15, 18, 19]. To the best of our knowledge, no pressure-induced bulge test measurements on polyimide membranes for screen-printed inks have been found in literature. While this work focuses on circular membranes to retrieve Young's modulus and residual stress of the film, shape variations, specifically high aspect ratio rectangles, could be used to extract other parameters such as Poisson's ratio [14, 15, 17, 19].
- Nanoindentation consists in probing a material with a tip of a specific well-known shape that is pressed into it while measuring the needed force, the depth and the stiffness [20, 21]. Based on those measurements and an assumption of Poisson's ratio, several characteristics from the material can be extracted among which, Young's Modulus using the Oliver & Pharr model [20]. In the case of films, the substrate influence on the measured characteristics can be minimized if specific requirements are met: (i) the measurement depth is less than 10% of the film thickness, and (ii) as a consequence of the small depth, a low roughness is necessary to minimize the experimental spreading due to depth measurement errors [22]. This work presents inks with low roughness (bellow 1 µm) and nanoindentation is used for comparative measurements with the bulge test as the technique is very standard for film mechanical characterization.

Measuring the inks mechanical characteristics with the deposition and curing conditions that will be used in further processes is of interest, as the thick films properties are sensitive to a large set of parameters. The section Materials and Methods describes the sample fabrication process for the membranes and their screen-printed coating, followed by the measurement setup for bulge test with a white light interferometer coupled to a pressure chamber. The fabrication of the samples and the setup for the comparative nanoindentation measurements finish this section. In the results section, the deflection profiles of the membranes, measured by interferometry, are described, along with the method and hypotheses used for the analysis to retrieve Young's modulus and internal stress of the ink layer. The nanoindentation results are also given in that section. The discussion challenges the results from the bulge test in regards of the values obtained with the nanoindentaiton. The hypotheses and requirements of both methods are also analysed regarding the fabrication and measurements reality.

MATERIALS AND METHODS

In this work, two inks that can be used in development of future sensing structures printed on flexible membrane are investigated. The first screen-printing ink is a custom blend of two products from DuPont with a 60/40 weight ratio. The reference 7082M [8], a conductive carbon-based ink designed for piezoresistive applications, is combined with the reference 3571 [9], an insulating dielectric polymer-based ink. The weight ratio of the blend allows to control the electrical resistivity range, starting from 1.7 Ω c for pure 7082M resistive carbon-ink and increasing with addition of the dielectric blend member 3571 up to above 100 kΩ cm. The second ink is a conductive ink with silver nanoparticles fillers with the reference Smart Screen F (S-CS21303) from Genesink [10]. The inks are denominated DuPont Carbon Blend (DCB) and Genesink Silver (GS), respectively, in the rest of this work.

The samples studied in this work are two-layers membranes whose top layer is the cured screen-printed ink of interest. As a pressure difference ΔP is applied between the two sides of the membrane, it deforms along. This deflection h is conditioned by two main characteristics: the overall tension $\sigma_{0,stack}$ and the rigidity R_{stack} of the full stack of materials composing the membrane:

$$\Delta P = \frac{4t}{a^2}\sigma_{0,\text{stack}}h + \frac{8t}{3a^4}R_{\text{stack}}h^3, \tag{1}$$

with ΔP the pressure difference applied between the front side of the membrane (at atmospheric pressure) and the cavity at its backside, t the membrane thickness and a the membrane radius, as indicated in Figure 1 [23]. The rigidity R_{stack} can be expressed as a function of Young Modulus E and Poisson's ratio ν, with the assumption that tangential and radial stresses are equal all over the membrane [23], as follows:

$$R_{\text{stack}} = \frac{E_{\text{stack}}}{1 - \nu_{\text{stack}}}. \tag{2}$$

Sample fabrication

Silicon wafers are chosen as the starting material to realize membranes of well-controlled sizes anchored on a rigid substrate. The fabrication process of the samples is kept as standard as possible to be highly reproducible, versatile, and low-cost. The first step is to grow a layer of wet thermal oxide of about 100 nm on standard

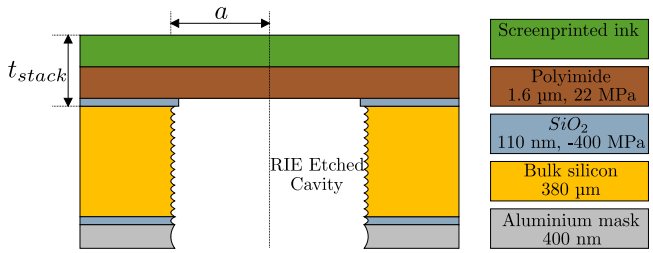

FIGURE 1 Schematic section view of the produced polyimide membranes: the top layer (green) is the ink, either DuPont Carbon Blend or Genesink Silver, that is screen-printed on the membrane structure. The released membrane is made of the spincoated polyimide layer (brown), while the oxide layers (blue) serve as sacrificial stop layer for the frontside and hardmask for the backside, the aluminum backside mask (gray) is needed to have a correct quality for the reactive ion etching (RIE) of the cavity in the bulk silicon (yellow). The circular membranes have a radius *a* variing from 0.75 to 2 mm and a total thickness t_{stack} depending on the screen-printed layer.

3-inch CZ wafers. This layer is used as a stop layer for subsequent silicon etching. Next, the polyimide precursor PI2545 is spincoated on the front side at 5000 rpm and cured following a curing cycle of 60 min at 200°C and 60 min at 350°C under a nitrogen flux. An aluminum layer of 400 nm is evaporated on the backside to serve as a hard mask. Both aluminum and silicon dioxide layers are patterned with a standard photolithography step followed by H_3PO_4 and BHF liquid etchings, respectively. The silicon substrate is then etched through the backside openings using a reactive ion etching process until the SiO_2 stop layer is reached.

Once the membranes are released, half of the wafers are coated with DCB and the remaining ones with GS. A continuous layer is screen-printed through a polyester mesh of type 120-34 cm/DIN (120 mesh elements per centimeter, with a thread of 34-µm diameter) with a large 10×10 cm^2 opening and cured directly on the processed wafer. Each of the two inks is then cured in specific conditions: (i) the DCB ink is cured at 150°C for 30 min and (ii) a 170°C curing for 30 min is used for the GS ink. The section view of the sample with the different layers is illustrated in Figure 1.

The curing procedure provokes large changes in stresses and initial deformation of all membrane layers. As temperature is increased, the membrane buckles to a large extent inside the cavity, due to the differences in thermal dilatation coefficients and stress release temperatures between polyimide and silicon dioxide. First, the thermal expansion coefficients are ranging from 30 to 60 [10^{-6}/K] for polyimide [24] and 0.55 to 0.75 [10^{-6}/K] for silicon dioxide [25]. Second, the temperatures of 150 to 170°C applied during ink curing are high enough to partially release stresses in the polyimide layer, while it does not significantly affect the silicon dioxide. This provokes further buckling as the stresses are no longer tensile across the full stack and become compressive due to the oxide layer. The combination causes the shattering of the oxide layer, which flakes away.

The final two-layers membranes are composed of the polyimide coated with the chosen ink, respectively DCB or GS. They are of circular shape with radius ranging from 1 to 2 mm for the DCB ink and 0.75 to 1 mm for GS-coated ones. During the cool-off period after curing, residual stresses in the polyimide layer are restored, leaving the membranes in a tensile state [26].

Bulge measurement setup

The wafers are cleaved into dies of 1×1 cm^2 and each is glued on a unpatterned printed circuit board (PCB) used as rigid supporting plate with a hole that is aligned with the back of the membrane. The M-BOND 200 adhesive kit, from Micro-Measurements, combines a glue with a catalyst to form thin and sealed layers.

The PCB are then inserted in a small pressure chamber setup that allows to impose a pressure difference between the two sides of the membrane by controlling the pressure inside the chamber relatively to the atmospheric pressure, P_{atm}. The pressure chamber consists of a body with access to a differential pressure device, to apply the pressure delta ΔP, as represented in Figure 2. It is covered by a plate and both are mechanically clamped together by bolts. To ensure pressure control underneath the membrane, two O-rings seal the cavity from the ambience. This setup is displayed in Figure 2a.

A white-light interferometer MSA-500 from Polytec is used to measure the topography of the sample die without physical contact

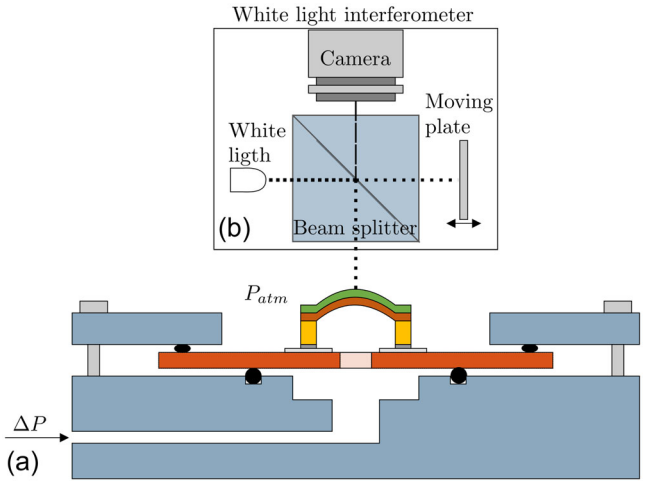

FIGURE 2 Schematic view of the setup for topography measurement of a membrane in deflection under pressure. (a) The membrane sample glued is on a printed circuit board (red) with pressure hole (transparent red), clamped in the pressure chamber setup with the body and the covering plate (blue) joined together (gray) and sealed with O-rings (black). The outside of the pressure chamber is at atmospheric pressure P_{atm} while the inside is controlled at a ΔP from P_{atm}. (b) The topography measurement is taken with a white light interferometer. The principle sketch shows the white light source, the beam splitter with the beams trajectories to the moving plate and the imaged sample. The camera captures the interference pattern between the splitted beams reflections.

to extract the curvature of the membrane. The principle is illustrated in Figure 2b. A white light source emits a ray that goes through a beam splitter and is separated into a reference beam projected onto a moving plate and the reflected beam towards the sample. The camera captures the interference between the reflections of both beams on their target, which occurs when the moving plate is at the same distance from the beam splitter than the reflection on the sample surface. The topographic image of the membrane is formed by moving the interferometer plate and focus along the *z*-axis [27]. The interferometer Polytec MSA-500, in Topography Measurement System (TMS) mode, can measure the deflection of the membrane with a precision down to 15 nm, over a maximum vertical range of 250 µm [28].

Nanoindentation control measurements

To compare the results on membranes with a state-of-the-art technique, nanoindentation essays of each ink are performed on bulk substrate. Standard 3-inch CZ silicon wafers are chosen as substrate, since the measurement on films works best if Young's modulus of the film is inferior to that of the substrate, $E_{film} < E_{substrate}$ [22]. Unpatterned inks layers are directly screen-printed on the bare silicon wafers, using the same screen and conserving the same printing parameters on the machine as in Section 2.1. The wafers of both processes, i.e. for bulge test or for nanoindentation, are then cured together in the same oven. Even though only the base layer changes from the polyimide film to the bare silicon, the ink layer can be impacted, especially in terms of thickness and microstructure. Hence, the thickness and roughness of the ink layers have been measured by profilometry for both processes. The wafers are then cleaved into dies of approximately $1 \times 1\,cm^2$. Those dies are indented in 16 spots positioned as a 4×4 matrix with 75 µm pitch. Nanoindentation measurements are performed on an Agilent G200-XP head equiped with a diamond Berkovich tip. The continuous stiffness mode at 45 Hz was chosen and the substrate effect is decorrelated using the Hay and Crawford model [22]. The values were taken between 9.5% and 10.5% of film thickness for both inks.

RESULTS

Thickness uniformity is an important parameter in both bulge test and nanoindentation. The samples on which the layer is non-uniform upon visual inspection were therefore left out except for one for discussion and comparison purposes. The curvature profiles measured on membranes under pressure with interferometry are visible in Figure 3, that shows the 1-mm radius membrane coated with DCB ink. The raw profiles are corrected by substracting the tensile profile at 0 kPa to suppress the measurement artefacts that can occur on the edges of the membranes. A second-order polynomial fit can be used to extract the maximum deflection h_{max}, according to the theory of

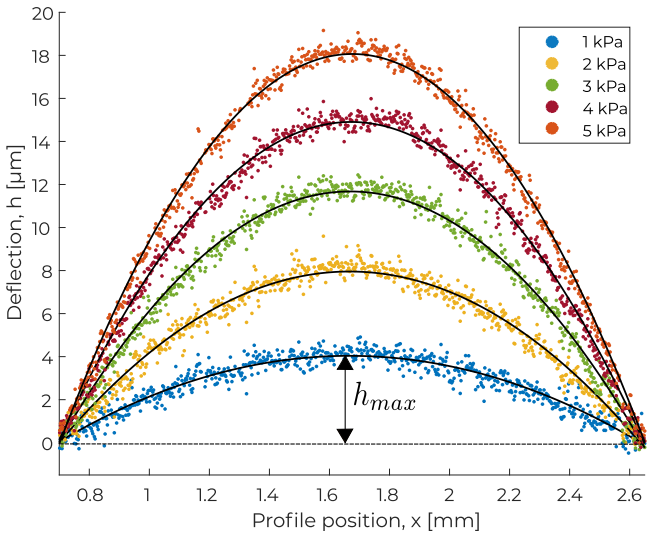

FIGURE 3 Deflection profiles obtained by interferometry for a 1-mm-radius membrane coated with DuPont Carbon Blend ink, corrected by subtraction of the profile at 0 kPa. The curvature of the membrane is fitted by a second-degree polynomial to extract the maximal deflection h_{max}, at the center of the membrane.

circular membrane deflection [23]. The maximum deflection h_{max} is the peak value, as indicated in Figure 3 which corresponds to the absolute value the polynomial's second derivative.

The relationship between the pressure applied on the membrane and the deflection shape can then be fitted using a polynomial of the form $\Delta P = \alpha h + \beta h^3$ as Equation (1). The measurements points and corresponding fitted curve for a membrane of 1 mm radius coated with DCB are displayed in Figure 4a. Both the linear, in Figure 4a, and cubic, in panel b, components can then be considered separately. By identification with Equation (1), the coefficient of the linear term, α, allows to extract the residual stress of the stack as $\sigma_{0,stack} = \alpha\frac{a^2}{4t}$, while the β constant from the cubic term directly yields its rigidity, using $R_{stack} = \beta\frac{3a^4}{8t}$. The results for the measured membranes are given in the columns $\sigma_{0,stack}$ and R_{stack} of Table 1.

From the rigidity of the membrane, the stack's equivalent Young's Modulus E_{stack} is estimated under two hypotheses: (i) the Poisson ratio is considered to be $\nu = 0.35$ for both the polyimide and the ink in the bi-layer stack and (ii) the equivalence of radial and tangential stresses [23] for a circular membrane deflection is supposed valid and Equation (2) is used. The corresponding values for each measured sample are given in Table 1, under E_{stack}.

Last, the internal stress of the ink itself $\sigma_{0,ink}$ and its Young's modulus E_{ink} can be retrieved under the hypothesis that the behavior of a material stack is close to the average of the different layers, weighted by their thicknesses [29]. The values extracted from the bulge test are given in Table 1 in the corresponding $\sigma_{0,ink}$ and E_{ink} columns. This step supposes that the thicknesses of all the stack's layers are known as well as the other layer's material parameters, here their Young's modulus and residual stress. The values used for the polyimide layer's Young's modulus is

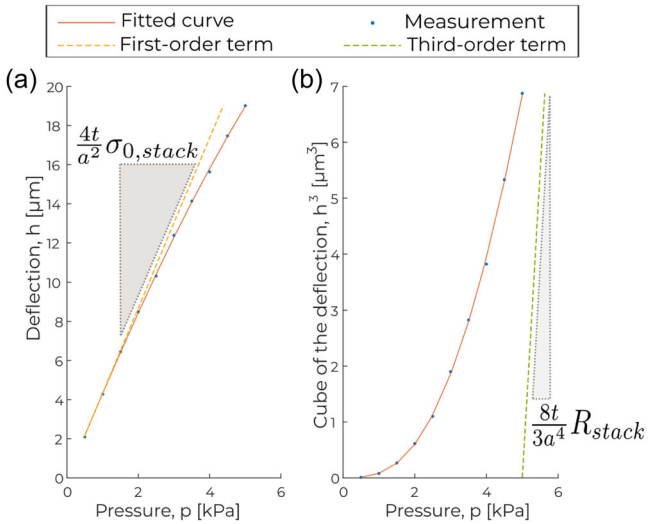

FIGURE 4 Comparison between measurement points (blue dots), third-order fits (see Equation 1) (red line) and linearisations (dashed lines) for a 1-mm DuPont Carbon Blend-coated membrane: (a) Deflection in function of pressure, with the linear component depending on the stress (yellow dashed line), (b) Cube of the deflection in function of pressure, with the third-order component depending on the rigidity of the material (green dashed line).

TABLE 1 Results extracted from the fitted pressure-deflection measurements by interferometry, for the different membranes measured with both DuPont Carbon Blend (DCB) and Genesink Silver (GS) inks.

Ink	a [mm]	$\sigma_{0,stack}$ [MPa]	$\sigma_{0,ink}$ [MPa]	R_{stack} [GPa]	E_{stack} [GPa]	E_{ink} [GPa]
DCB	1	12.9	8.0	7.7	5.0	6.2
	1.5	10.2	3.9	9.3	6.1	7.8
	2	5.4	−3.6	7.6	4.9	6.0
GS	0.75	5.8	−13.6	3.2	2.1	1.9
	1	6.4	−8.9	10.8	7.5	12.1

Note: The extracted values are the residual stress of the full stack $\sigma_{0,stack}$, the internal stress of the ink layer $\sigma_{0,ink}$, the rigidity of the membrane R_{stack}, Young's moduli of the full stack E_{stack} and the ink E_{ink}.

E_{PI} = 2.3 [GPa] [30]. Its residual stress measured using a standard Stoney procedure on full wafer [31, 32] during fabrication is 21.8 MPa. The Stoney procedure consists in monitoring the full wafer curvature changes through profilometry measurements at each process step and extracting the internal stresses of the deposited layers in function of the curvature delta.

Table 2 presents the profilometry measurements of the ink layers and the results obtained with nanoindentation of the same inks. The profilometry measurement of thickness t and roughness r gave similar results for both processes, with the base layer being either silicon or polyimide. E_{ink} is Young's modulus of the ink evaluated by nanoindentation. Its value is an average over the 16 indents, with the corresponding standard deviation (SD).

DISCUSSION

The obtained results for Young's modulus determined with the bulge test are validated by comparison with the values from nanoindentation. Furthermore, the bulge test presents the advantage to enable measurements of the mechanical properties directly in the conditions of operation of the material, in the perspective of producing MEMS with released parts. Several assumptions can be discussed, such as the values of several material parameters, the expression of the dependence to the value of Poisson's ratio v and the averaging of material characteristics along the stack of materials in the membrane.

(i) The first hypotheses in measurement processing are the values of the material parameters of the PI layer and Poisson's ratio of the full stack. The Young's modulus of the polyimide layer is considered to be 2.3 GPa and its Poisson's ratio 0.35 according to datasheets. Since the polyimide layer is spincoated from a precursor, its properties can therefore present some variations with regard to the datasheet specification [30]. For Poisson's ratio, the value is supposed to be close to 0.35 for both inks. This value is estimated based on the behavior of polymers as they are polymer based [33]. The same value was used for both the processing of membrane-based measurements and nanoindentation results. (ii) The second hypothesis is the equality of tangential and radial stresses over the membrane that yields Equation (2). In literature, models for deflection based on finite elements analysis from Pan et al. [34] and from Tabata [17] propose different expressions for $R_{stack} = E_{stack} f(v)$ with a higher-order dependency to v. In this work, since the value of v is not measured, considering a more complex function of v would not increase significantly the confidence in the exact values of the results for Young's Modulus. (iii) The last hypothesis for data treatment to discuss, is the consideration that a stack of material can be approximated as the weighted average of the different layers. This neglects any type of interactions between the different layers or any directional gradient.

The matching between the extracted results and the nanoindentation proves the reliability of the bulge test method as long as those assumptions are valid. The values obtained for the membranes coated with DCB with a radius of 1- and 2-mm fall within the standard deviation around the nanoindentation mean value. The 1.5-mm radius membrane falls within the interval of two to three times the standard deviation. Part of the reasons for such variation might be small thickness deviation due to device-to-device variation and the sensitivity of those inks to atmospheric conditions, especially

TABLE 2 Thickness t and roughness r of the ink layer measured by profilometry and distribution of the nanoindentation results for Young's Modulus E_{ink} with the associated standard deviation (SD).

Ink	Thickness t [μm]	Roughness r [μm]	E_{ink} [GPa]	SD [GPa]
DCB	2.9	1	5.48	0.93
GS	1.6	0.6	30.31	5.04

Abbreviations: DCB, DuPont Carbon Blend; GS, Genesink Silver.

humidity, which might cause changes in thickness and residual stresses. Differences in the microstructures between the samples printed on polyimide and silicon could also explain those differences, even though it was not explored in this work.

The membranes coated with GS give results with a much lower Young's modulus than the values from the nanoindentation test, by a factor 2 to 3. This difference could be explained by several factors: the first, as in the two examples cited in the introduction, is a difference in the effective curing conditions and the second is the change of substrate from polyimide to silicon that can impact the thickness in various ways. The variation in effective curing conditions, even though conditions were the same wafer-wise, is coming from the fact that the layer deposited on membranes is effectively cured on a 1.5 µm thick layer of polyimide above a cavity whereas the one on silicon is cured directly on a substrate of 380 µm. Right after curing of the membrane-based samples, an intense buckling is observed, causing the shattering of the stop layer oxide. Spontaneous stress and strain restoration has been observed, and the membranes go back to a tensile state. In literature, Young's modulus of silver films treated with the drying-sintering combination have been measured between 44 and 48 GPa through nanoindentation [3] and around 14 GPa for a deflected cantilever [4]. The explanation of that difference is linked to sintering conditions and the porous nature of the silver layer [4]. Even though the typical sintering temperatures (above 700°C) would be destructive for polyimide membranes, differences in microstructures of the silver ink layer could also arise in the present curing conditions.

Thickness variations can impact strongly the results as deflection is proportional to a constant thickness value according to Equation (1). However, changes in the screen printing conditions can also provoke variations of the ink layer thicknesses: a different substrate with different surface energy can cause irregularities or the presence of edges will provoke the formation of menisci. Figure 5 compares layer uniformity condition and membrane behavior in deflection. Figure 5a shows the topography and profilometry measurement of the 1.0-mm radius GS coated membrane and Figure 5b shows the measured deflection profile. Two small menisci can be seen at the edge of the membrane but the surface is generally smooth, hence the correct fit of the deflection profile. The 0.75-mm radius membrane that was coated with GS shows the topography and profilometry

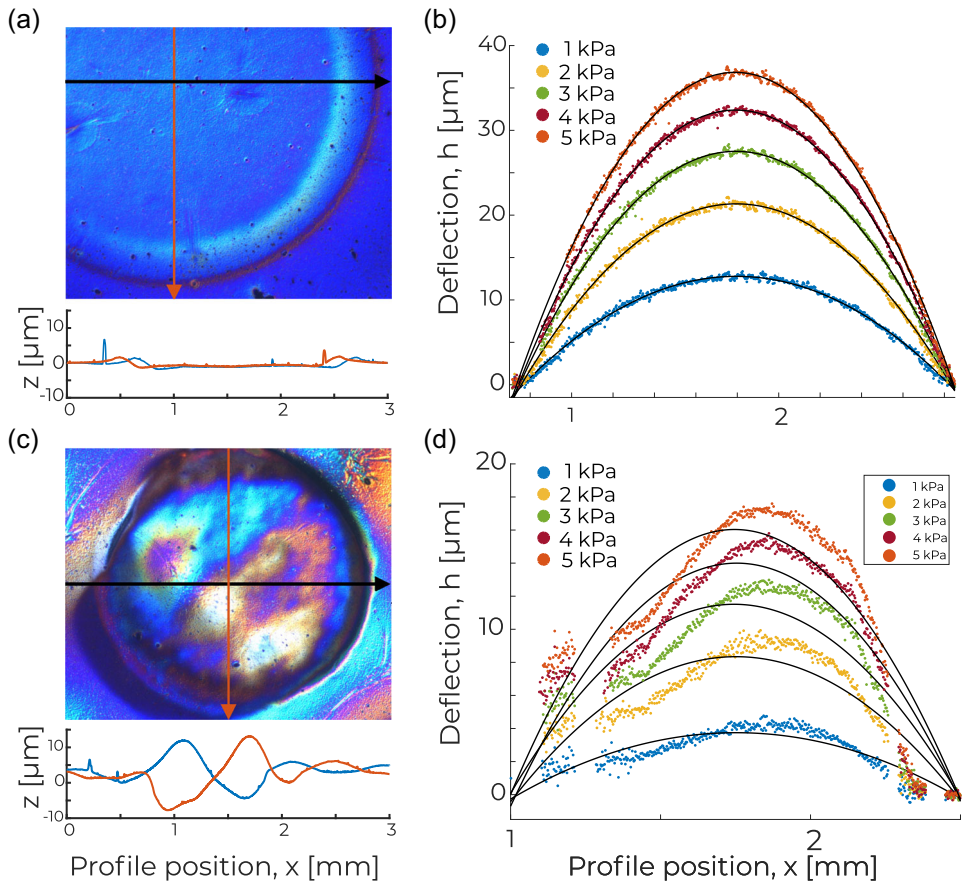

FIGURE 5 Comparison between valid and invalid samples regarding the uniform ink thickness hypothesis: (a) valid sample, 1.0-mm radius membrane with Genesink Silver (GS) ink layer, with the profilometry measurements underneath along two axes, vertical (red) and horizontal (black), (b) the deflection along the horizontal axis with the second-order fit, (c) invalid sample, 0.75-mm radius membrane with GS ink layer, with the profilometry measurement showing ink build up to 15 µm, and (d) the corresponding deflection results with a second-order polynomial fit. The thicker zone of the membrane deflects less and the overall profile is not aligned with the quadratic fit.

measurement from Figure 5c. The hills and valleys build up to 15 µm. As the blue profilometry curve from Figure 5c is taken along the same axis as the profile from Figure 5d, the side with the ink accumulation deflects less than the other. This causes the interferometry results for that membrane to not correspond to a shape that can be correctly fitted with a second-degree polynomial as observed in Figure 5d. The method is therefore not suitable for measuring samples where the thickness nonuniformity causes the membrane deflection to show strong deviation from the quadratic model.

The obtained results for the stack internal stress $\sigma_{0,stack}$ are directly extracted from the fit, as shown in Figure 4a. The tensile values correspond with the observation of flat membranes when no pressure is applied on their backside. The value of the stress in the ink is retrieved using the model of averaging of stresses over the full stack. In the case of the DCB ink, the values for its residual stress $\sigma_{0,ink}$ are decreasing as the membrane radius increases, becoming compressive for the largest. This could be linked to the intensity of the deflection during the curing of the ink layer. Regarding the GS layers, the extracted values are compressive as well. The value obtained for the 0.75-mm membrane is submitted to the same cautions as its Young's modulus value as the thickness discussions are also valid here.

CONCLUSION

Polyimide membranes on silicon substrate coated with screen-printed ink showed the possibility to measure their deflection under pressure to retrieve Young's modulus and residual stress of the screen-printed different layer. A third-order fit of the curvature interferometry measurements is used to extract Young's modulus of two screen-printed inks: a carbon-based resistive blend and a silver nanoparticle ink, which respectively yield values of 6–8 and 12 GPa. The residual stress spans −3.6 to 8.0 MPa for the carbon-based blend and is around −10 MPa for the silver one.

The differences observed with nanoindentation results, both from state-of-the-art and specific to this work, can be explained by two main reasons: estimated values for Poisson's ratio and dependency of the deflection model to that value on one side; variations in the deposition and curing conditions on the other. For residual stresses values, the variations could be correlated with membrane size and the expansions and retractions due to curing and cool-off. The exact fabrication process for both membrane-based samples and nanoindentation ones is thoroughly detailed. This allows to point out that (i) the substrate has impact on the layer during the deposition step, as surface energy is conditioning the ink spread and can change thickness, and (ii) curing on a thin layer of material above a cavity is different from curing on a solid substrate, as the thin membrane can deform under heat treatment. For future investigations of screen-printed elements on membranes, those points are critical to ensure correct designs, simulations and fabrications of hybrid MEMS.

ACKNOWLEDGMENTS

The authors thank Audrey Favache for the nanoindentation measurements and Benoît Hubert for the pressure measurement setup adaptations. They also thank Nicolas André for his precious advice about the fabrication process. This work was supported by the CAPFLEX project funded by Wallonia Region, Belgium.

CONFLICT OF INTERESTS STATEMENT

The authors declare no conflict of interest.

DATA AVAILABILITY STATEMENT

The data that support the findings of this study are available from the corresponding author upon reasonable request.

ORCID

Eléonore Masarweh http://orcid.org/0000-0003-4025-565X

REFERENCES

[1] M. Prudenziati, *Sens. Actuators A* **1991**, *25*(27), 227.
[2] M. Hatala, P. Gemeiner, M. Hvojnik, M. Mikula, *J. Mater. Sci. Mater. Electr.* **2018**, *30*, 1034.
[3] D. Paretkar, N. J. Glassmaker, K. Mikeska, G. Blackman, A. Jagota, *IEEE J. Photovoltaïcs* **2016**, *6*(5), 1141.
[4] R. Lakhmi, H. Debeda, I. Dufour, C. Lucat, 20th Workshop Micromachining, Micro Mech. Micro Syst. (MME'09), Toulouse, France, **2009**.
[5] J. Izdebska, in *Printing on Polymers: Theory and Practice* (Eds: J. Izdebska, S. Thomas), Plastic Designs Library Series, Elsevier, **2016**, 1–20.
[6] S. Tepner, N. Wengenmeyr, M. Linse, A. Lorenz, M. Pospischil, F. Clement, *Adv. Mater. Technol.* **2020**, *5*, 2000654.
[7] R. Maas, M. Koch, N. Harris, N. White, A. Evans, *Mater. Lett.* **1997**, *31*, 109.
[8] DuPont de Nemours, *DuPont 7082M Carbon Conductor*, **2021**.
[9] DuPont de Nemours, *Blend Member/Dielectric - Polymer Thick Film Composition*, **1997**, Rev 11.95.
[10] Genesink *Smart Screen F (S-CS21303) Product Data Sheet*, **2019**, Rev 07.
[11] A. Yunos, G. Omar, M. Salim, N. Masripan, M. HussinAhmedAl-Mola, *Int. J. Nanoelectr. Mater.* **2020**, *13*, 431.
[12] Metallic materials–sheet and strip–determination of biaxial stress-strain curve by means of bulge test with optical measuring systems, standard, International Organization for Standardization, Geneva, CH, **2022**.
[13] E. Obermeier, Talk at materials research society symposium, San Francisco, **1997**.
[14] J. Vlassak, W. Nix, *J. Mater. Res.* **1992**, *7*(12), 3242.
[15] S. Shafqat, O. van der Sluis, M. Geers, J. Hoefnagels, *Thin Solid Films* **2018**, *660*, 88.
[16] F. Bahrami, M. W. Malik, F. Van Loock, J.-P. Raskin, T. Pardoen, B. Nysten, *Meas. Sci. Technol.* **2023**, *34*(12), 125027.
[17] O. Tabata, T. Tsuchiya, *IEEJ Trans. Sens. Micromachines* **1996**, *116*(1), 34.
[18] M. Orthner, L. Rieth, F. Solzbacher, *Rev. Sci. Instrum.* **2010**, *81*, 055111.
[19] J. Mitchell, C. Zorman, T. Kicher, S. Roy, M. Mehregany, *J Aerospace Eng.* **2003**, *16*, 46.
[20] W. Oliver, G. Phar, *J. Mater. Res.* **1992**, *7*(6), 1564.
[21] W. Oliver, G. Phar, *J. Mater. Res.* **2003**, *19*(1), 3.
[22] J. Hay, B. Crawford, *J. Mater. Res.* **2010**, *26*(6), 727.

[23] W. Schomburg, *Introduction to microsystem design—RWTH Edition*, Aachen, Springer, **2011**.
[24] S. Numata, S. Oohara, J. Imaizumi, N. Kinjo, *Polym. J.* **1985**, *17*(8), 981.
[25] Materials A. Silica-silicon dioxide (SiO_2) **2023**. https://www.azom.com/properties.aspx?ArticleID=1114. Accessed September 10, 2023.
[26] H. Chung, Y. Joe, H. Han, *J. Appl. Polym. Sci.* **1998**, *74*(14), 3287.
[27] Polytec, White-light interferometry, **2023**, https://www.polytec.com/eu/surface-metrology/technology/white-light-interferometry (accessed: September 2023).
[28] Polytec, Hardware manual micro system analyser msa 500, **2010**.
[29] J. Laconte, Micromachined thin-film sensors for SOICMOS co-integration. PhD thesis, Université catholique de Louvain, **2004**.
[30] H MicroSystems*Product bulletin PI-2545 Wet Etch Applications*, **2009**.
[31] G. Stoney, *Proc. R. Soc. A* **1909**, *82*(553), 172.
[32] G. Janssen, M. Abdalla, F. van Keulen, B. Pujada, B. van Venrooy, *Thin Solid Films* **2009**, *517*, 1858.
[33] G. Cahn, A. Barrios, S. Graham, J. Meth, A. Antoniou, O. Pierron, *Materialia* **2020**, *10*, 100642.
[34] J. Pan, P. Lin, F. Maseeh, S. Senturia IEEE 4th Technical Digest on Solid-State Sensor and Actuator Workshop, Hilton Head, SC, USA, **1990**.

How to cite this article: E. Masarweh, M. Arseenko, P. Guaino, D. Flandre, *Appl. Res.* **2024**, e202300113. https://doi.org/10.1002/appl.202300113